Discrete Modeling of Fluid-Particle Interaction in Soils

Jidong Zhao* and Tong Shan

Department of Civil and Environmental Engineering, Hong Kong University of Science and Technology, Clearwater Bay, Kowloon, Hong Kong
jzhao@ust.hk

Summary. Fluid-particle interaction contributes to important behaviors of soils. This paper presents a numerical method to model the interaction by coupling the Computational Fluid Dynamics (CFD) with the Discrete Element Method (DEM). The particle motion of the granular system is simulated by the DEM, and the CFD solves the locally averaged Navier-Stokes equation for the flow of pore fluid. The interaction between pore fluid and particles is considered by exchange of interaction forces between DEM and CFD. The numerical method is further benchmarked and validated by several geomechanics problems.

Keywords: fluid-particle interaction, CFD, DEM, sandpile.

1 Introduction

Fluid-particle interaction underpins the key behavior of granular soils in many applications. Conventional approaches have been based on continuum, phenomenological theories of porous media and cannot offer important information at the microscale governing the interacted system of particles and fluid. While the microscopic behavior of the fluid-particle interaction may provide insights to the overall understanding of granular materials, a coupled CFD-DEM numerical tool will be developed in this study to simulate the fluid-particle interactions in granular soils.

2 Formulation and Approach

In a particle system simulated by the DEM, the following equations are assumed to govern the translational and rotational motions of a particle:

$$\begin{cases} m_i \dfrac{\mathrm{d}\mathbf{U}_i^p}{\mathrm{d}t} = \displaystyle\sum_{j=1}^{n_i^c} \mathbf{F}_{ij}^c + \mathbf{F}_i^f + \mathbf{F}_i^g \\ I_i \dfrac{\mathrm{d}\boldsymbol{\omega}_i}{\mathrm{d}t} = \displaystyle\sum_{j=1}^{n_i^c} \mathbf{M}_{ij} \end{cases} \tag{1}$$

* Corresponding author.

Q. Yang et al. (Eds.): Constitutive Modeling of Geomaterials, SSGG, pp. 297–301.
springerlink.com

where $\mathbf{U}_i^p$ and $\boldsymbol{\omega}_i$ denote the translational and angular velocities of particle i, respectively. $\mathbf{F}_{ij}^c$ and $\mathbf{M}_{ij}$ are the contact force and torque acting on particle *i* by particle *j* or walls, and n_i^c is the number of total contacts for particle i. $\mathbf{F}_i^f$ is the particle–fluid interaction force acting on particle *i*, which include both buoyancy force and drag force in the current case. $\mathbf{F}_i^g$ is the gravitational force. m_i and I_i are the mass and moment of inertia of the particle. The Hooke contact law in conjunction with Coulomb's friction law is employed to describe the interparticle contact behaviour. For the fluid system, the following continuity equation and locally averaged Navier-Stokes equation will be solved by the CFD:

$$\begin{cases} \dfrac{\partial(n\rho)}{\partial t} + \nabla\cdot\left(n\rho\mathbf{U}^f\right) = 0 \\ \dfrac{\partial\left(n\rho\mathbf{U}^f\right)}{\partial t} + \nabla\cdot\left(n\rho\mathbf{U}^f\mathbf{U}^f\right) - n\nabla\cdot\left(\mu\nabla\mathbf{U}^f\right) = -n\nabla p - \mathbf{f}^p + n\rho\mathbf{g} \end{cases} \tag{2}$$

where $\mathbf{U}^f$ is the average velocity of a fluid cell, ρ is averaged fluid density. n defines the porosity (void fraction). p is the fluid pressure in the cell; μ is the averaged viscosity; $\mathbf{f}^p$ is the interaction force averaged by the cell volume the particles inside the cell exert on the fluid. $\mathbf{g}$ is the body force vector.

The drag force and buoyancy force are considered to be the dominant interaction forces between fluid and particles for low Reynolds number pore flows. The following expression is employed for the drag force (see [1-2]):

$$\mathbf{F}^d = \frac{1}{8}C_d\rho\pi d_p^2\left(\mathbf{U}^f - \mathbf{U}^p\right)\left|\mathbf{U}^f - \mathbf{U}^p\right|n^{1-\chi} \tag{3}$$

where d_p is the diameter of the considered particle. C_d and χ depend on the Reynolds number of the considered particle $\mathrm{Re_p}$

$$C_d = \left(0.63 + \frac{4.8}{\sqrt{\mathrm{Re}_p}}\right)^2,\quad \chi = 3.7 - 0.65\exp\left[-\frac{\left(1.5 - \log_{10}\mathrm{Re}_p\right)^2}{2}\right] \tag{5}$$

and $\mathrm{Re}_p = n\rho d_p\left|\mathbf{U}^f - \mathbf{U}^p\right|/\mu$.

The buoyancy force adopts the following expression:

$$\mathbf{F}^b = \frac{1}{6}\pi\rho d_p^3\mathbf{g} \tag{6}$$

The general computational scheme is outlined as follows (see also [3]). The fluid phase is discretized with a typical cell size five to ten times of the average particle diameter. At each time step, the DEM package will provide such information as the position and velocity of each individual particle. The position of each particle is then matched with the fluid cell to calculate relevant information of each cell such as the porosity. Eq. (2) is solved by the CFD program for the averaged velocity and pressure for each cell. The obtained averaged velocity and pressure of a cell are then used to determine the drag force and buoyancy force acting on the particles within the cell. Iterative schemes may be required to ensure the convergence of relevant quantities such as fluid velocity and pressure. When a converged result is obtained, the information of the fluid-particle interaction forces will be taken into account for the next step calculation of the DEM part. Ideally, information on interaction forces should be exchanged once after each step of calculation for DEM or CFD. This, however, may be computationally extremely expensive in practice. For most problems, numerical experience indicates that for each CFD computing step, exchange of information after every 100 steps of DEM calculation will ensure sufficient accuracy as well as efficiency. If the time steps for DEM and CFS are sufficiently small, more steps for DEM are also acceptable.

3 Benchmarking and Application

Two classic geomechanics problems are first employed to benchmark the proposed CFD-DEM method. One is the one-particle settling in water problem, and the other is the one-dimensional consolidation problem. Analytical solutions to both problems are available in soil mechanics text books. Predictions by the numerical tool for the two problems are compared against the analytical solutions in Figure 1.

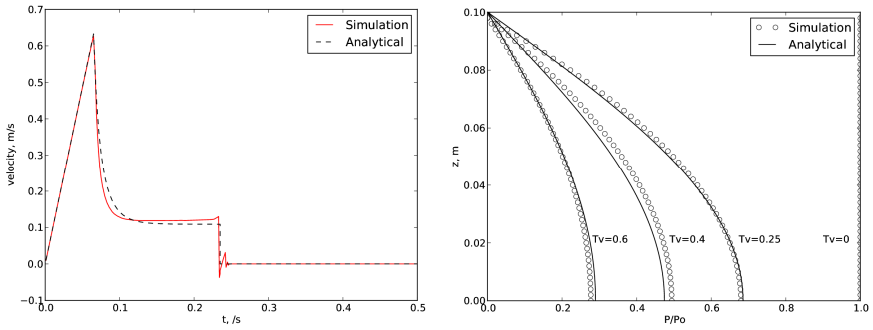

(a) (b)

Fig. 1. Benchmarking of the CFD-DEM method with analytical solutions for (a) the single-particle settling in water problem; (b) one-dimensional consolidation problem

For the single particle settling problem, it is evident from Figure 1a that the settling velocity of a sphere particle in water predicted by the CFD-DEM agrees well with the analytical solution. Sharp reduction of settling velocity of the particle when it hit the water is accurately captured, along with the settling process in the water. The bounce back from the bottom of the contained is also reproduced well. For the 1D consolidation problem, Figure 1b shows that the simulated dissipation of excess pore water with time also compare reasonably well with the analytical solution. However, it is also noticed (not shown here) that at very early stage of consolidation, i.e., when $T_v < 0.1$, the numerical prediction deviates slightly from the analytical solution. This is because the Terzaghi's analytical solution assumes an instantaneous build-up of excess pore pressure throughout the column once the surcharge is applied, whereas the CFD-DEM calculation needs some time to build up the excess pore water.

The CFD-DEM method has also been applied to investigating the formation of sandpile in water. Shown in Figure 2a demonstrates the formation process of a sandpile in water through hopper flow. The case without water has also been simulated for comparison. Meanwhile, the rolling resistance has been regarded important in simulating the sandpiling problem (see [4]), and will be considered here. Presented in Fig. 2b is the pressure dips observed in sandpiles obtained in the various cases. The overall profile of the vertical pressure in the wet case is higher than the dry case. The pressure dip is found to be moderately reduced by the presence of water as compared to the dry case. Consideration of rolling resistance may lead to enhanced pressure dip, and the difference is more appreciable in the wet case than in the dry case. From a further inspection of the force chain network it is found that the presence of water may lead to more homogeneous contact force distribution in the sandpile, which may help to explain the reduced pressure dip in the wet.

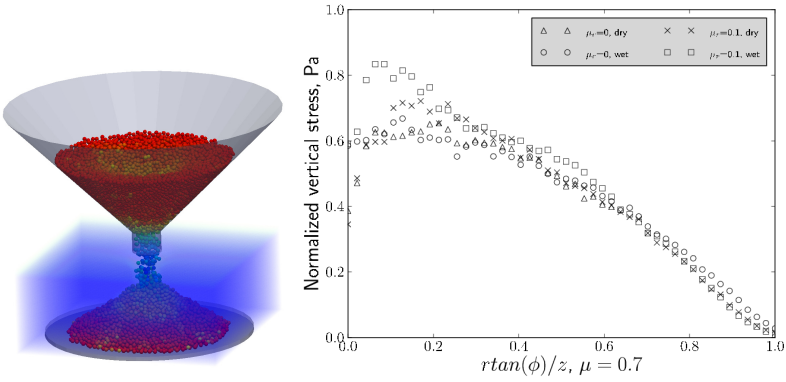

(a) (b)

Fig. 2. CFD/DEM simulation of sandpiling in water. (a) Schematic of forming a sandpile in water through hopper flow; (b) Comparison of pressure dip in sandpiles formed in dry/wet conditions and with/without consideration of rolling resistance.

5 Conclusion

A CFD-DEM numerical tool has been developed to simulate the fluid-particle interaction in granular soils. It was benchmarked by two classic geomechanics problems and was further applied to the sand pile formation in water. It is shown that important behavior of fluid-particle interaction in soils can be well captured.

Acknowledgement. The work was supported by Research Grants Council of Hong Kong (GRF 622910).

References

[1] De Felice, R.: The voidage function for fluid-particle interaction systems. Int. J. Multiphase Flow 20(1), 153–159 (1994)
[2] Zhu, H., Zhou, Z., Yang, R., Yu, A.: Discrete particle simulation of particulate systems: Theoretical developments. Chemical Engineering Science 62(13), 3378–3396 (2007)
[3] O'Sullivan, C.: Particulate Discrete Element Modelling: A Geomechanics Perspective. Spon Press (an imprint of Taylor & Francis), London (2011)
[4] Zhou, Y.C., Wright, B.D., Yang, R.Y., Xu, B.H., Yu, A.B.: Rolling friction in the dynamic simulation of sandpile formation. Physica A 269, 536–553 (1993)